

Reply to referee 1

We thank the referee for the comprehensive and constructive review which helped a lot to revise the manuscript. Below please find our point-by-point reply to the comments which are repeated here in shaded boxes.

This work described how the mixing of dust and pollution aerosol changes dust optical and radiative properties by increasing its extinction and reducing its absorption. Furthermore it quantifies the change in radiative effect of natural dust at the top of the atmosphere, at the surface and in the atmospheric column. A short discussion of regions where the mixed dust cools or warms the atmosphere over 4 regions is also included. To be worthy of being published in ACP, this paper needs to give a reasonable amount of details on how the dust cycle is treated, what are the assumptions under which acids can be uptaken by dust and give the limitation of the optical properties derived by mixing dust with other aerosols. Here are the elements to add to this work to place it in the context of what has already been published on dust.

We have included more details on the implementation of the dust cycle, the condensation of acids and the aerosol optical properties in section 2 of the revised manuscript.

Ridley et al., 2016 and Kok et al. (2017) that you cite have established constraints on the dust cycle using both satellite observations and 3 independent models. Please state the amount of total yearly emissions, the yearly mean total optical depth and total deposition flux of dust in your model and compare them to these constraints.

In the revised manuscript we discuss these numbers in the last paragraph of the methodology section.

How do you represent the particle size distribution (PSD) of dust. The PSD has a large influence on the value of your LW radiative effect. You should state how large a particle you represent and what fraction of dust particles suspended are PM₁, PM₁₀, or above 10 microns for example.

We have added information on the modal size distribution to the methodology section. One indicator for a realistic size distribution are the comparisons with AOD observations at different wavelengths shown in Fig. S1 in the supplement.

Then, when you account for the uptake of acids by dust, please state which acids, which chemical species you consider, and what accommodation coefficients were chosen. No need to refer the reader to another paper, a simple Table can go a long way to help the reader navigate through your assumptions of uptake coefficients.

We have added Table 2.

Other major points include:

Page 2, between the 2 last paragraphs of this page it would be welcome to state the main questions that you are trying to answer in this paper. After reading the introduction, the reader should be fully aware in what directions the paper will take him or her.

We inserted a new paragraph.

Page 3, line 26: The reader needs to know what refractive indices you took for dust both in the SW and in the LW, please state simply your reference for them and whether these refractive indices are coherent with AERONET observations or indicate a dust that is too absorbing compared to these measurements.

We have added the sources of all refractive indices used by the AEROPT submodel and added the refractive index figure and tables from the supplement of Klingmueller et al. (2014) to the supplement.

Page 3, line 26. You state that you assume spherical particles and make an hypothesis of volume averaged refractive index when mixing particles. There is abundant literature that this approximation is invalid and that a dielectric or a Maxwell-Garnett approximation describes better the state of mixture of an aerosol. State why you made this choice and what is the error associated with it.

Using the volume average refractive index is the EMAC default mixing rule and has been applied in previous studies on which the present study is based. More importantly, comparing various mixing assumptions in EMAC (Klingmueller et al., 2014), where the optical properties integrate a large range of Mie size parameters and particle compositions, showed that using the Maxwell-Garnett mixing rule does not much change the results. In addition, in the same study the average refractive index mixing rule tends to yield optical properties closer to that of core-shell particles than the Maxwell-Garnett mixing rule. Considering that under certain conditions core shell particles represent real particles (in particular dust after the uptake of water) more closely than homogeneous mixed particles, there is no clear advantage in using the Maxwell-Garnett mixing rule for our application.

Minor points:

In the abstract please state that you treat both dust radiative effect both in the SW and LW range of the spectrum.

This is mentioned in the revised abstract.

A Figure showing as a function of wavelength the refractive indices used separately for the SW and LW would be very useful to the reader.

We have added the refractive index figure and tables from the supplement of Klingmueller et al. (2014) to the supplement.

Page 5 line 20: could you find any field measurements that could guide you as to whether the hygroscopic variations of dust that the model represents are well captured?

The model representation of the hygroscopic variations has been evaluated against field measurements by Metzger et al. 2016. Abdelkader 2017 evaluated the chemical ageing during the transatlantic dust transport using ground based AERONET observations and satellite retrievals from MODIS and CALIPSO. Consistent results were also reported by other studies (e.g., Abdelkader 2015, Klingmueller et al. 2018, Bruehl et al. 2018).

Page 7 line 8: typo Change: “The distribution of the bottom of the atmosphere (BOA) forcing (Fig. 4, bottom) is similar to the that of the TOA forcing,” with “The distribution of the bottom of the atmosphere (BOA) forcing (Fig. 4, bottom) is similar to that of the TOA forcing,”

This has been fixed in the revision.

Page 7, line 25; I am expecting that for region 1 Figure 5 would show a cooling effect for the atmospheric column. On this Figure, the heating rates are positive at almost all heights, how one can reconcile this fact with an overall cooling effect?

The profiles depicted in pale colours are the heating rates caused by dust which is now explicitly mentioned in the caption. The heating rates due to the interactions are negative (blue).

Page 8, lines 11 and 12: please give separately the contributions of the SW and the LW to the pollution free dust radiative effect of $-0.08 \text{ W} \cdot \text{m}^{-2}$ and to the polluted dust of $-0.13 \text{ W} \cdot \text{m}^{-2}$.

We have added the SW and LW contributions.

I believe that this paper can be vastly improved if you account for these recommendations.

References: Kok, J. F., Ridley, D. A., Zhou, Q., Miller, R. L., Zhao, C., Heald, C. L., Ward, D. S., Albani, S., and Haustein, K.: Smaller desert dust cooling effect estimated from analysis of dust size and abundance, *Nat. Geosci.*, 10, 274–278, <https://doi.org/10.1038/ngeo2912>, 2017. Printer-friendly version

Ridley, D. A., Heald, C. L., Kok, J. F., and Zhao, C.: An observationally constrained estimate of global dust aerosol optical depth, *Atmos. Chem. Phys.*, 16, 15097–15117, <https://doi.org/10.5194/acp-16-15097-2016>, 2016.

We use both references in the revised manuscript.

Reply to referee 2

We thank the referee for the thorough and constructive review. We have revised the manuscript accordingly. Please find below the point by point reply to the individual comments.

General comment

This manuscript investigates how microphysical and chemical interactions between dust and pollution alters the properties of aerosols and their direct radiative effects (DRE). The experimental design is simple and effective. A set of four simulations have been used to model the properties of aerosols when dust and pollution are either emitted separately, or together so that they interact. By contrasting results from these simulations the study reveals the “interaction” term showing how the properties of the dust and the pollution-related aerosol change due to two-way microphysical and chemical interactions. It is interesting to explore such interactions and the changes in aerosol radiative effects are not trivial, so worth noting.

The main result is that the dust-pollution interactions lead to a -0.05 Wm^{-2} change in net flux at TOA, dominated by increased SW reflection. This occurs mainly due to increases in accumulation-mode aerosol mass and AOD. The AAOD also drops slightly, though it is not completely clear why, though it is perhaps related to a drop in coarse-mode dust. As climate models and Earth-system models are increasingly adopting more complex microphysical aerosol schemes it is worthwhile understanding what happens as such interactions are enabled. To my knowledge this manuscript is novel and I would judge it to be relevant and worth publishing in ACP. The text is generally well written, well structured and concise. However, significant improvements in the analysis and interpretation of the results are required for the study to be published.

Major comments

The main difficulty with this manuscript is that it is not very clear what has caused the negative change in aerosol DRE. The text interprets this as a change in dust forcing, or an “anthropogenic radiative forcing associated with dust”. However, the dust-pollution interaction is a two-way process and changes both the dust and the fine-mode anthropogenic aerosols. Figures S11, S12, S13 indicate significant changes to the “pollution-related” aerosol once the dust and pollution are emitted together so one can not attribute the change in DRE entirely to the dust.

Indeed the interaction is a two-way process and technically we treat both directions equally as manifested by Eq. (2). The interpretation as a change in dust forcing is motivated by the fact that historically the dust was there before the pollution and therefore the pollution modified the already existing dust forcing. In contrast, the opposite case where dust is added to pollution never occurred on global scale. Therefore and to make the discussion of the results more comprehensible, we use this interpretation as guiding principle but nevertheless discuss the impact of dust on pollution. The term “anthropogenic radiative forcing associated with dust” is supposed to reflect that the effect is linked to (but not solely attributed to) dust and at the same time anthropogenic because of the anthropogenic origin of the pollution.

The main cause of the negative change in aerosol DRE seems to be the increases in accumulation-mode aerosol, but it is not very clear from the study which aerosol components have contributed to this increase. More information is required to show how the aerosol properties have changed, including changes in aerosol mass, chemical composition, hygroscopicity, and possibly particle size across the relevant size modes.

The increase of the accumulation-mode burden is caused by mineral dust due to the reduced coagulation with coarse particles in the presence of pollution. The accumulation mode-burden of other components is generally reduced due to the increase of coagulation in the presence of dust, exceptions are the ions (Fig. S11, now S12). The increase of accumulation mode dust dominates in dusty regions, resulting in a net-increase of the accumulation-mode burden. We have added figures showing the interaction effect on dust, BC, SS and water burdens separately to the supplement and discuss them in the main text.

Related to this, it is not very clear what has caused the changes in AAOD and SSA. Presumably AAOD reduces in dusty regions due to a drop in coarse-mode mass? The AAOD increases across the Sahel are apparently due to increases in BC and OC mass (lifetime) but it would be good to see the evidence to support this. However, it isn't clear why the SSA drops in non-dusty regions that are quite remote from dust sources. Presumably there is a relative reduction in non-absorbing aerosol components such as sulphate and/or nitrate, but why does this occur in regions very remote from dust. There are some clues in Figure S11 but there are many competing effects and the information is not comprehensive enough to understand what it going on.

The AAOD reduction in dusty regions is mainly caused by the change of the accumulation mode composition in the presence of dust which transfers absorbing carbonaceous components from the accumulation to the coarse mode. This becomes more clear from the new aerosol component burden plots in the supplement. On the other hand the increased accumulation mode dust increases the AAOD, this effect dominates south of the Sahel to produce a net AAOD increase. In contrast, over Asia where not only the burden of absorbing components but also the AOD decreases, both effects reduce the AAOD so that a negative net effect is obtained even relatively remote from dust sources. Additionally, as you mention, in dusty regions the coarse mode mineral dust and hence an absorbing component is reduced, which further contributes to the AAOD decrease.

The other major concern I have is the short duration of the simulations (only one year). Given the episodic nature of dust emissions there is likely to be considerable interannual variability in dust loadings and in how these interact with pollution outbreaks. This could affect both the magnitude and spatial patterns of the results. I would recommend extending the simulations to least a 10 years, unless the authors can provide evidence that a single year is sufficient to gauge the magnitude and characteristics of the dust-pollution interactions.

Despite the episodic nature of dust emissions the global annual averages presented here are relatively robust regarding interannual variations which is confirmed by a lower resolution sim-

ulation over 10 years that yields coefficients of variation (CV) for our main results below 10 %. Therefore, even though the results are explicitly presented for 2011, they are considered representative for recent years. We have added a paragraph to the methodology section and CV estimates to the caption of Fig. 6.

Minor comments

Abstract: The abstract is short and direct but needs to be altered to reflect the concerns above. In particular, the change in aerosol DRE is described as a “radiative forcing” here and throughout the manuscript. This could be confusing or misleading as the term “forcing” is usually used to indicate a change in radiation balance due to a perturbation in aerosol emissions. The ΔF is really more “the change in aerosol DRE due to dust-pollution interactions”. This could be given a label such as ΔDRE_{int} to avoid using this long definition each time in the text.

While a “forcing” is often attributed to emissions, it is not uncommon to assign a forcing to other effects such as changes in the solar irradiance, surface albedo changes or cloud adjustments due to aerosols. Especially the latter, the forcing of aerosol-cloud interactions, bears similarities to the forcing by dust-pollution interactions so that we consider using the term “forcing” in our context to be not exceptionally confusing.

P1 L5: Please spell out EMAC.

We have expanded the acronym.

P1 L7: Whilst the magnitude of the change in TOA radiation balance is worth noting, I would not describe it as large. In fact it is quite small compared to the total DRE of aerosol in present-day climate (~ -2 to -3 Wm^{-2}).

We have deleted “large”.

P1 L10: Please quantify this “considerable fraction”.

We have quantified the fraction (40 %).

Methods: P3 L10: It is not quite clear what the term “prognostic radiative-transfer calculations” means. Presumably this is the radiative-transfer calculations that are used to calculate fluxes and heating rates in the simulations. Using “prognostic” is a bit confusing since the prognostic aerosols are clearly not used in the radiation scheme, and a radiation scheme is not itself prognostic.

We have reformulated to “the aerosol radiative effect on the dynamics is computed using the extinction, single scattering albedo and asymmetry factor from the Tanre aerosol climatology”.

P3 L13: Is the dynamical evolution of the atmosphere (wind, temperature, moisture, cloud) identical in all four simulations? I would have thought so if the prognostic aerosols neither interact with the clouds or the radiation scheme.

Yes, they are identical which is now mentioned in the discussion of Eqs. (1) and (2) in section 2.

P4 L17-18: I think that you need to swap $F_2 - F_4$ and $F_3 - F_4$ in this sentence. From my reading of the text $F_3 - F_4$ corresponds to the dust radiative effect and $F_2 - F_4$ corresponds to the pollution.

This has been fixed in the revision.

P4 L23: So it sounds like a radiation double-call procedure has been used, as outlined in Ghan et al. (2012). <https://journals.ametsoc.org/doi/10.1175/JCLI-D-11-00650.1> If so it might be useful to reference Ghan et al. (2012) as this paper outlines the double-call concept fully.

We have added the reference.

Results: P5 L20 / Fig 1: Does the mass shown in Fig 1 include the aerosol water content?

Yes (we have added a note in the caption of Fig. 1).

Figures 1 – 3: Exactly how are the differences in mass and optical properties calculated? Are these calculated using the same logic as in equation 1?

Figures 1 and 2 are calculated using Eq. (1). Fig. 3 shows the difference of the SSA results from the simulation with (simulation 1) and without pollution (simulation 3) (both simulations include dust). Equation (1) cannot be used to study the effect on the SSA since the SSAs of dust and pollution are not additive when neglecting the interaction.

P5 L24: Would it be possible to provide a figure for the dust mass loading, or at least refer to Figure S1 here so the author can see where the “dust affected regions” are simulations.

We have added the reference to Fig. S1.

Section 3: I found this section difficult to follow (particularly the top half of P6) and it did not provide a full explanation of how / why the aerosol properties changed.

P6 L7-9: This argument needs explaining more fully. It is clear that the coarse mode dust is removed more rapidly due to secondary aerosol forming on the particles leading to more rapid wet deposition. However, what happens to the accumulation mode dust? Wouldn't the same process also speed the removal of the accumulation mode dust compared to the simulation where pollution was not emitted with the dust? From figure S11 it looks like the overall mass of sulphate and nitrate aerosol in the accumulation-mode has decreased. So this would tend to decrease accumulation-mode mass and the hygroscopicity, yet total accumulation-mode mass and AOD have increased. Presumably the mass of BC and OC must have increased dramatically to compensate the decreases in sulphate and nitrate. Is there evidence of this? It would be good to see all the relevant mass components in figure S11 and have the full story explained.

Compared to the coarse mode, an additional sink for the accumulation mode is the coagulation with coarse particles, which is less efficient in the polluted simulation 1 than in simulation 3 without pollution (due to the more efficient removal of coarse particles). Therefore simulation 1 produces more accumulation mode dust particles than simulation 3 despite a more efficient deposition. This difference dominates Eq. (1) resulting in the burden increase displayed in Fig. (1). We have added the corresponding plots for mineral dust, black carbon, sea salt and water individually in Fig. S12 in the supplement, showing that the accumulation mode burden increase is due to dust.

P6 L25-26: The SSA has reduced in most non-dusty regions. Is this due to an increase in the relative proportion of BC and/or OC versus sulphate and nitrate? Why would this have occurred even in regions very remote from dust? It would be good to provide a table listing the global-mean values and global mean changes in relevant quantities, such as AOD, AAOD, radiative flux changes and the various aerosol mass components.

Please note that Fig. 3 does not show the result of Eq. (1) but the SSA difference between simulation 1 with pollution and simulation 3 without pollution. The negative values very remote from dust result from adding pollution including absorbing BC and OC to the mostly non-absorbing natural background aerosol (e.g., sea salt, water). Since the natural aerosol burden can be very low compared to the burden from pollution, the SSA difference in remote regions is not very relevant (hence the colour scale cut-off at -0.012). Because global means integrate compensating effects and large areas unaffected by dust, regional values are more informative (the relevance of the global TOA forcing for the climate's energy budget make it an exception), accordingly we have added a table with regional mean values and the corresponding contributions of the dust-pollution interactions for relevant quantities.

P6 L20: How has the aerosol become more reflective? I suspect the drop in AAOD is dominated by the decline in coarse-mode dust mass so I would omit "due to the higher reflectance" from this sentence.

The water which is taken up by the aged hygroscopic dust particles reduces the average imaginary

refractive index of the particles, increasing the reflectance.

P6 L21. The AAOD is presumably increased in the Sahel due to increased BC mass (and brown carbon if this is included in the model). The explanation that this is due to AOD increase doesn't make sense, only one can say that both may be increasing for similar reasons.

The AAOD is proportional to the AOD (for constant SSA), thus an increase of the AOD increases the AAOD.

Conclusions: The main concerns given above need to be addressed throughout the conclusions. The change in aerosol DRE can not be interpreted as a change in dust forcing as it is caused by both changes in dust and pollution aerosol properties. The conclusions section is very concise, which is good, but a bit more discussion is required to explain what has caused the changes in aerosol DRE, and how these are linked to aerosol processes and changes in aerosol properties (mass, hygroscopicity, optical properties etc).

While we agree that the impact of dust on pollution is crucial which is now emphasized more throughout the revised manuscript, the change in the forcing is by definition the change of the dust forcing which occurs when pollution is added to the natural scenario (see Eq. (1)). Mathematically this is identical to the change of the pollution forcing when adding dust to a dust free scenario ($(F_1 - F_3) - (F_2 - F_4)$). However, as mentioned above, this never occurred in the real world on a global scale, therefore we consider the interpretation as change in dust forcing to be more instructive. We have added a paragraph summarising the causes of the changes in aerosol forcing.

P8 L20: The maximum impact to the south of the Sahel is given as -2.5 Wm^{-2} here but -2 Wm^{-2} in the abstract. From reading closer I see this is because the -2.5 Wm^{-2} quoted here corresponds to the surface forcing and the abstract gives the TOA forcing. Please use the same headline result in abstract and conclusions.

We have included the TOA result in the revised conclusions.

Figures: There are a lot of additional figures in the supplementary material and some offer an unnecessary level of detail on the spatial and seasonal variability of aerosol radiative effects (S5, S9, S15, S19 - 23). Given that the spatial distributions and seasonality of results are probably very specific to the model and the meteorological evolution in this specific set of simulations, this level of detail is not particularly useful and could be misleading. The 3D visualizations of aerosol heating in particular are not at all useful.

It is true that due to the shorter underlying time period the seasonal results have a higher statistical uncertainty and are less representative for the same season of other years. But since the meteorology is nudged towards reanalysis data, the meteorological evolution in the simulations agrees well with observations and so do the aerosol concentrations which is supported by many previous studies (e.g., Pozzer et al. 2012, Abdelkader et al. 2015, 2017, Metzger et al. 2016, Klingmueller et al. 2018). Therefore we consider the seasonal results to be not specific to the sim-

ulations but well representative for the year 2011. Given the seasonality of dust emissions we assume the seasonal results are valuable to some readers and prefer to retain most of the figures while removing the 3D plots.

Figure S11: As expressed above, to really understand how the dust-pollution interaction affects aerosol properties this figure needs to include changes in OC, BC, dust, water and sea salt. The figure may need expanding to two or three figures to give a complete summary of the changes in aerosol mass and composition.

Figure S11 focusses on the main aerosol ions which interact with the mineral cations in the dust and are in exchange with precursor gasses shown in the same figure and therefore play a distinct role. The revised supplement additionally includes the Figures for dust, BC, SS and water burdens separately (Fig. S11) and a discussion in the main text. Qualitatively the same effect as for BC is obtained for OC but no OC coarse mode model output is available.

Figure S12 & S13: It is quite interesting to have this kind of information, but it was rather difficult to interpret how the mass of dust, pollution, water and natural aerosols change between the three scenarios. It would be clearer to have just one bar for each emission scenario (all emission, no pollution, no dust) and have each bar stacked showing the relevant mass components (dust, pollution, water and other natural aerosol). This way it would be totally clear how each mass contribution has changed depending on what has been emitted. It is still very interesting to provide this separately for both the accumulation and coarse-modes. Would it be possible to produce this kind of figure also for the global mean changes? As this analysis is really quite important to the story of the paper it would also be worth considering moving this (especially a plot with global-mean changes) to the main article.

Figures S12 and S13 are closely related to Eq. (2), the “No dust” and “No pollutions” bars are stacked to allow a direct comparison of the term corresponding to $(F_2 - F_4) + (F_3 - F_4)$ with the term corresponding to $F_1 - F_4$. We have straightened the figure by stacking the mass contribution bars, but still stacking the “No dust” and “No pollution” values and moved it to the main article. This is complemented by a new figure in the supplement showing regional burdens (which are more useful than global averages) with one bar per simulation as proposed.

Figure 6: This graph really emphasizes the interpretation that the dust-pollution interaction has strengthened dust forcing, which is misleading since the interaction has also altered the strength of the anthropogenic (pollution) aerosol forcing. For a more balanced summary it would be good to include a bar for the forcing from pollution and bars for “Dust + pollution with interaction”, and “Dust + pollution without interaction” instead of the bar with “Dust interacting with pollution”.

As argued above, while we agree that the interpretation as a change in dust forcing is not the only interpretation possible, we consider it to be a valid and well motivated perspective. Aside from this the comparison with the dust forcing works better due the similar magnitude. The underlying reason is that for both, the interaction and the dust forcing, regional contributions

compensate each other. The pollution forcing is discussed in section 2.

Relevant changes

In response to the referee comments the following changes have been implemented:

Manuscript

- The main text has been expanded throughout the document (please see the latexdiff output below for details)
- One figure has been added (Fig. 2)
- Two tables have been added (Tables 2 and 3)
- The following references have been added: Brühl et al. 2019, Dietmüller et al. 2016, Feng et al. 2007, Ghan et al. 2012, Gómez-Amo et al. 2017, Hanisch and Crowley 2003, Hess et al. 1998, Huneus et al. 2011, Kerkweg et al. 2006a, Kirchstetter et al. 2004, Koepke et al. 2015, Raes and Van Dingenen 1992, Ridley et al. 2016, Rothman et al. 2005, Stier et al. 2005, Tost et al. 2006, Van Doren et al. 1990, Vignati et al. 2004

Supplement

- Two figures have been added (Figs. S11 and S20)
- Figures S12 and S13 have been replaced by the new Fig. S13
- Figures S20 to S23 have been removed
- Two tables have been added (Tables S1 and S2)

The following latexdiff output details the changes in the main text.

Direct radiative effect of dust-pollution interactions

Klaus Klingmüller¹, Jos Lelieveld^{1,2}, Vlassis A. Karydis^{1,3}, and Georgiy L. Stenchikov⁴

¹Max Planck Institute for Chemistry, Hahn-Meitner-Weg 1, 55128 Mainz, Germany

²The Cyprus Institute, P.O. Box 27456, 1645 Nicosia, Cyprus

³Forschungszentrum Jülich GmbH, IEK-8, 52425 Jülich, Germany

⁴King Abdullah University of Science and Technology, Thuwal 23955-6900, Saudi Arabia

Correspondence: Klaus Klingmüller (k.klingmueller@mpic.de)

Abstract. The chemical ageing of aeolian dust, through interactions with air pollution, affects the optical and hygroscopic properties of the mineral particles and hence their atmospheric residence time and climate forcing. Conversely, the chemical composition of the dust particles and their role as coagulation partners impact the abundance of particulate air pollution. This results in an anthropogenic radiative forcing associated with mineral dust notwithstanding the natural origin of most aeolian dust. Using the [ECHAM/MESSy](#) atmospheric chemistry climate model ~~EMAC-with-(EMAC)~~, [which combines the Modular Earth Submodel System \(MESSy\) with the European Centre/Hamburg \(ECHAM\) climate model, including](#) a detailed parametrisation of ageing processes and an emission scheme accounting for the chemical composition of desert soils, we study the direct radiative forcing globally and regionally [considering solar and terrestrial radiation](#). Our results indicate **large** positive and negative forcings, depending on the region. The predominantly negative forcing at the top of the atmosphere over large parts of the dust belt, from West Africa to East Asia, attains a maximum of about -2 W/m^2 south of the Sahel, in contrast to a positive forcing over India. Globally averaged, these forcings partially counterbalance, resulting in a net negative forcing of -0.05 W/m^2 , which nevertheless represents a considerable fraction [\(40 %\)](#) of the total dust forcing.

1 Introduction

Atmospheric aerosols play an important role in the climate system by affecting radiative transfer and thus the planet's energy budget, both directly by scattering and absorption and indirectly via its impact on cloud formation (IPCC, 2014). Furthermore,

fine particulate matter can be a human health hazard and is a major cause of morbidity and mortality globally (Lelieveld et al., 2015).

Aerosols originate both from natural and anthropogenic sources, the former being mostly mineral dust, sea salt and emissions from naturally ignited fires. Mineral dust is the dominant aerosol component by mass and natural sources are responsible for most of its atmospheric load, even though about 25 % may be from ~~man-made~~ human-made sources (Ginoux et al., 2012). The natural sources provide an inevitable background level of atmospheric particulate matter, while studies of the human impact on climate and air pollution commonly focus on aerosol from anthropogenic sources. However, within the atmosphere natural and anthropogenic aerosols are mixed and interact, and therefore should not be considered separately.

In the presence of anthropogenic pollution, gaseous compounds, notably acids, condense on the mineral dust particles (Karydis et al., 2011). The consequent interactions are dubbed chemical ageing, converting the initially hydrophobic dust particles into hydrophilic ones (Karydis et al., 2017), leading to the hygroscopic growth of the particles with implications for their optical properties and the rate of deposition (Levin et al., 1996; Abdelkader et al., 2015, 2017). The dust particles also serve as coagulation partners for particulate anthropogenic pollution. Moreover, the chemical composition of the dust particles affects the chemical properties of the aerosol mixture (Karydis et al., 2016) and hence the hygroscopic and optical properties as well as the atmospheric residence time of both the natural and anthropogenic components. In view of emerging economies with growing population and increasing emissions from industry, energy production and transport in dust affected regions such as northern Africa, the Middle East and large parts of Asia, the importance of these effects is ever-increasing (Osipov et al., 2015; Osipov and Stenchikov, 2018).

In the present study we analyse the impact of mineral dust interactions with anthropogenic air pollution on radiative transfer using the ECHAM/MESSy chemistry climate model (EMAC) (Jöckel et al., 2005, 2010). EMAC combines the Modular Earth Submodel System (MESSy) with the ~~ECMWF~~ European Centre/Hamburg (ECHAM) climate model which is originally based on the weather forecasting model of the European Centre for Medium-Range Weather Forecasts (ECMWF). Here we focus on the direct radiative effects while not considering aerosol cloud coupling, and ignoring radiative feedbacks on the climate system. Both aspects, of which especially the former influences radiative forcing, will be considered in a separate study based on climate model simulations that account for atmosphere-ocean coupling.

Our main goal is to understand how the mineral dust in the present day atmosphere differs from dust under natural conditions and in particular to evaluate the implications on the global and regional radiative transfer, which is the focus of the present study. Accordingly we choose the methodology described in the following section which, in contrast to previous studies (Abdelkader et al., 2015, 2017), does not alter the chemical ageing mechanism but rather the emissions. The impact of dust

on pollution is crucial and therefore considered by our approach on an equal footing with the impact of pollution on dust. A technical objective of this study is to assess the error introduced in climate models if mineral dust and anthropogenic pollution are assumed to be coexisting without any interaction and thereby to point out the importance of taking the interactions into account.

5 The article is structured as follows: In section 2 we present our methodology including the model setup-up. The effects of dust-pollution interactions on the aerosol burdens and correspondingly the optical properties are analysed in section 3, the resulting impacts on radiative transfer and atmospheric heating in section 4. Conclusions are drawn in section 5.

2 Methodology

We ~~use~~used the EMAC model version and configuration described by Klingmüller et al. (2018), which was shown to yield
10 realistic results of aerosol optical properties globally (see Fig. S1 in the supplement). This EMAC version combines ECHAM 5.3.02 and MESSy 2.52 and is configured to use the horizontal resolution T106 and 31 vertical levels. The grid spacing of the Gaussian T106 grid, 1.125° along latitudes and about 1.121° along longitudes, at the equator corresponds to virtually quadratic cells with around 125 km edge length. The following MESSy submodels have been enabled: AEROPT, AIRSEA, CLOUD, CLOUDOPT, CONVECT, CVTRANS, DDEP, GMXE, JVAL, LNOX, MECCA, OFFEMIS, ONEMIS, ORBIT,
15 ORACLE, PTRAC, RAD, SCAV, SEDI, SURFACE, TNUDGE, TROPOP. Descriptions of each submodel and further references can be found online in the MESSy submodel list (MESSy 2018). The model dynamics above the boundary layer are nudged to meteorological analyses of the European Centre for Medium-Range Weather Forecasts (ECMWF), and the ~~prognostic radiative transfer calculation uses the Tanre aerosol climatology for~~ aerosol radiative effect on the dynamics is computed using the extinction, single scattering albedo and asymmetry factor from the Tanre aerosol climatology (Tanre et al.,
20 1984). The aerosol radiative coupling to the meteorology, and that between aerosols and clouds have been disabled to exclude higher order effects such as feedbacks by precipitation and evaporation changes and to focus on the direct radiative forcing. The CMIP5 RCP4.5 (Coupled Model Intercomparison Project Phase 5 Representative Concentration Pathway 4.5) (Clarke et al., 2007), GFEDv3.1 (Global Fire Emissions Database) (Randerson et al., 2013) and AeroCom (Aerosol Comparisons between Observations and Models) (Dentener et al., 2006) databases provide anthropogenic, biomass burning and sea salt emissions,
25 respectively.

The EMAC model considers dust ageing by condensation of soluble compounds, ~~reactions into ionic species~~ ionization, hydrolysis and the associated water uptake. The model representation of the hygroscopic variations has been evaluated against field measurements by Metzger et al. (2016). Abdelkader et al. (2017) evaluated the chemical ageing during the transatlantic

dust transport using ground based AERONET (Aerosol Robotic Network) observations and satellite retrievals from MODIS (Moderate Resolution Imaging Spectroradiometer) and CALIPSO (Cloud-Aerosol Lidar and Infrared Pathfinder Satellite Observations). Consistent results were also reported by other studies (e.g., Abdelkader et al., 2015; Klingmüller et al., 2018; Brühl et al., 2018). The relevant submodels include the Global Modal Aerosol Extension (GMXE) (Pringle et al., 2010a, b), which simulates the aerosol micro-physics considering four soluble (nucleation, Aitken, accumulation, coarse) and three insoluble modes (Aitken, accumulation, coarse) employing. The size distribution of each mode is represented by a log-normal distribution with fixed geometric standard deviation ($\sigma_g = 2$ for the two coarse modes, $\sigma_g = 1.59$ for all others), fixed dry radius boundaries between the nucleation, Aitken, accumulation and coarse modes (6 nm, 60 nm and 1 μm) and variable mean radius. GMXE employs ISORROPIA II (Fountoukis and Nenes, 2007) or EQSAM4clim (Equilibrium Simplified Aerosol Model V4 for climate simulations) (Metzger et al., 2016) for the gas-aerosol partitioning (here we use the former). The amount of gas kinetically able to condense is calculated assuming diffusion limited condensation using the accommodation coefficients in Table 2 before ISORROPIA II re-distributes the mass between gas and aerosol phase to obtain the final amount of condensed material (Pringle et al., 2010a, b). The ORACLE (Organic Aerosol Composition and Evolution) submodel comprehensively describes organic aerosols (Tsimpidi et al., 2014). A detailed simulation of the gas phase chemistry is performed by the Module Efficiently Calculating the Chemistry of the Atmosphere (MECCA) (Sander et al., 2011).

Aerosol optical properties are calculated by the AEROPT (AERosol OPTical properties) submodel (Lauer et al., 2007; Pozzer et al., 2012; Klingmüller et al., 2014), which assumes the aerosol components within each mode to be well mixed in spherical particles with volume averaged refractive index. The refractive indices considered-AEROPT considers for the individual components are compiled from the OPAC 3.1 database (Hess et al., 1998) (black carbon, mineral dust), the HITRAN 2004 database (Rothman et al., 2005) (organic carbon, sea salt, ammonium sulphate, water), Kirchstetter et al. (2004) (organic carbon for $\lambda < 0.7 \mu\text{m}$) and additional mineral dust values for $\lambda > 2.5 \mu\text{m}$ (see Klingmüller et al., 2014). The full dataset is specified in the supplement of Klingmüller et al. (2014). A detailed simulation of the gas phase chemistry is performed by the Module Efficiently Calculating the Chemistry of the Atmosphere (MECCA) (Sander et al., 2011). (Fig. S25, Tables S1, S2). The imaginary part of the dust refractive index used here attains a minimum of $4 \cdot 10^{-3}$ at visible and near-infrared wavelengths. AERONET retrievals might yield lower values, e.g., Gómez-Amo et al. (2017) report 2.5 to $2.8 \cdot 10^{-3}$ over Spain, however due to ageing the modelled dust is usually mixed with other components and especially water so that the effective imaginary refractive index of the entire particles is lower than the value assumed for pure dust.

The dust emission scheme is evaluated-within-part of the online emission submodel ONEMIS (Kerkweg et al., 2006b). We use the dust emission scheme presented by Klingmüller et al. (2018) which is based on Astitha et al. (2012) and differentiates

the Ca^{++} , K^+ , Mg^{++} and Na^+ fractions in mineral particles originating from different deserts (Karydis et al., 2016). The majority of the mineral dust mass is emitted into the coarse mode (approximately 89 %), the remainder into the accumulation mode. Freshly emitted mineral dust is assumed to be hydrophobic and thus emitted into the insoluble modes. Only after condensation of sufficient soluble material to cover the particles with 10 monolayers or by coagulation with soluble particles,

5 initially insoluble particles are transferred to the soluble modes (Vignati et al., 2004; Stier et al., 2005; Pringle et al., 2010a, b). The removal by wet deposition is simulated by the scavenging submodel SCAV (Tost et al., 2006), dry deposition and sedimentation by the submodels DDEP and SEDI (Kerkweg et al., 2006a).

Our analysis covers the meteorological year 2011. Four simulations with varied emission setups (Table 1) are used to derive the instantaneous forcing by the interaction of mineral dust and anthropogenic pollution: one simulation considering all emis-

10 sions (simulation 1), the same simulation but without dust emissions (simulation 2), a simulation with only natural emissions (simulation 3) and the corresponding simulation without dust emissions (simulations 4). For the natural emission setups we omit the CMIP5 anthropogenic emissions and reduce the GFED biomass burning emissions by 90 % (Levine, 2014). All dust emissions are considered to be natural, hence the anthropogenic impacts of land use and climate change on the dust emissions (Klingmüller et al., 2016) are excluded from our analysis. The contribution of dust-pollution interactions to the total aerosol

15 radiative forcing can be calculated from the aerosol forcings $F_{1\dots 4}$ from the four simulations 1 to 4 by evaluating

$$\Delta F = (F_1 - F_2) - (F_3 - F_4), \quad (1)$$

the difference of the dust forcing with full emissions $F_1 - F_2$ and the dust forcing with only natural emissions $F_3 - F_4$. Analogously, we define the dust-pollution interaction effect on aerosol optical depth (AOD), atmospheric heating rates and aerosol particle burdens.

20 Note that the right hand side of Eq. 1 is symmetric regarding the exchange of dust and anthropogenic emissions, i.e., it considers the effect of the pollution on dust in the same way as the effect of dust on pollution by comparing the forcing of anthropogenic pollution in the presence of dust ($F_1 - F_3$) with its forcing in a dust free scenario ($F_2 - F_4$). Unlike the pollution free scenario, the globally dust free scenario has no counterpart in the real world, nevertheless this interpretation would be suitable to evaluate the regional impact of dust events or new dust sources on pollution. It can be instructive to

25 expand the ~~term~~ RHS of Eq. (1) to the difference of the combined dust and pollution forcing $F_1 - F_4$ and the sum of the forcing of only ~~dust-pollution~~ $F_2 - F_4$ and only ~~pollution-dust~~ $F_3 - F_4$,

$$\Delta F = (F_1 - F_4) - ((F_2 - F_4) + (F_3 - F_4)). \quad (2)$$

Due to clouds, radiative forcings strongly vary over time and accordingly their temporal averages are associated with substantial statistical uncertainty even for relatively long averaging intervals. ~~Calculating the~~ The computation of ΔF can be challenging if this uncertainty is uncorrelated between the individual terms $F_{1..4}$. If the aerosol-cloud and radiative coupling to meteorology are taken into account so that the cloud cover of the four simulations is no longer identical it is essential not
5 to use total fluxes on the RHS of Eq. 1 but to calculate the aerosol forcing as the difference between fluxes computed by two simultaneous radiative transfer computations, one with and one without considering the aerosol but both with identical cloud effect ~~-(Ghan et al., 2012; Dietmüller et al., 2016). This~~ eliminates most of the cloud related statistical noise. ~~This and~~ drastically reduces the length of the averaging period which is required to obtain significant results. Nevertheless, in the present study the cloud cover is identical for all four simulation because the different emission setups do not affect the meteorology.
10 To estimate the remaining statistical uncertainty, we split the time series of daily averages into n sub-samples, each consisting of only every n -th daily value. As long as the choice of n is not too large, this ensures that each sub-sample is unbiased by seasonality. We consider the random terms of the sub-samples to be largely uncorrelated, which allows the computation of the statistical uncertainty as standard error of the mean (SEM) of the results from all sub-samples. To obtain approximate uncertainty estimates, we use $n = 5$ for annual and $n = 7$ for seasonal analyses, which are small numbers with regard to the
15 SEM calculation but ensure representative subsets and are factors of the number of days per year and season, respectively. We use the resulting uncertainty estimate σ to apply a significance threshold of 2σ to our results. For our purpose, the one year simulation period turns out to be sufficient to produce significant results.

The interannual variation is estimated based on a 10 year simulation at lower T63 resolution (about 1.9°) which yields coefficients of variation (CV) below 10 % for our main results. We conclude that while the interannual variation is not negligible
20 it does not substantially affect our results. Other uncertainties such as biases in the parametrisations and emission inventories are likely more relevant. This especially applies to results which integrate partially compensating regional positive and negative contributions such as the change of the global top of the atmosphere (TOA) forcing by the dust-pollution interactions. EMAC yields similar results for different commonly used parametrisations of the optical properties of internally mixed particles (Klingmüller et al., 2014) so that the associated error is small as long as the particles are spherical which is the case after
25 hygroscopic growth. Considering non-spherical particles could improve the parametrisation for freshly emitted, dry mineral dust, but no substantial corrections are to be expected (Koepke et al., 2015).

The difference between the global direct aerosol radiative forcings in simulation 2 and simulation 4 yields an anthropogenic aerosol forcing of -0.61 W/m^2 at the ~~top of the atmosphere (TOA)~~ TOA (see Figs. S2 to S5 in the supplement), consistent with

the estimate of the aerosol-radiation interaction effective radiative forcing (ERF) of -0.45 (-0.95 to 0.05) W/m^2 indicated by IPCC (2014).

The global dust radiative forcing excluding the effect of dust-pollution interaction can be calculated as difference between the aerosol forcings in simulation 3 and simulation 4. At the TOA the net forcing amounts to -0.08 W/m^2 , comprising the solar radiation forcing of -0.16 W/m^2 and the terrestrial radiation forcing of 0.09 W/m^2 (see Figs. S6 to S9 in the supplement). The net forcing is less negative than the -0.14 W/m^2 reported by (Bangalath and Stenchikov, 2015), but well within the range of -0.48 to 0.20 W/m^2 estimated by Kok et al. (2017) and the wide spread of forcings from different models (Fig. S10 in the supplement, Yue et al. (2010), Table 1). The total yearly mineral dust emission and deposition rate is 1.31Gt/yr, slightly higher than the AeroCom estimate of 1.1Gt/yr (Huneus et al., 2011) and within the range 1.7 (1.0 to 2.7)Gt/yr provided by Kok et al. (2017). The global average 550 nm dust AOD of 0.021 is comparable to the AeroCom median of 0.023 (Huneus et al., 2011) but lower than the 0.03 ± 0.005 reported by Ridley et al. (2016). The relatively small dust AOD and forcings in the present study compared to previous work suggest that our estimates for the radiative effect of dust-pollution interaction which predominantly affects the solar spectrum may be considered as conservative.

3 Aerosol burdens and optical properties

The condensation of soluble compounds, their reaction and the consequent hygroscopic growth increase the size of the dust particles and thereby their dry deposition velocity and the efficiency of in- and below-cloud scavenging. Figure 1 (top) shows that the anthropogenic dust ageing significantly reduces the dust and hence the coarse mode annual mean mass burden throughout most dust affected regions -(the right column of Fig. S1 in the supplement highlights the relevant the regions). The only notable exception is over the western Atlantic Ocean. ~~After transport and mixing with African pollution, well aged Saharan dust takes up substantial amounts of water resulting in a regional increase of the coarse mode burden; elsewhere the hygroscopic growth does not compensate the burden decrease due to the more efficient removal.~~ Here, the mineral dust moderates the reduction of sea salt and the associated water by anthropogenic pollution.

The effect on the accumulation mode aerosol burden, being most relevant for the AOD and hence radiative transfer, is more complex because not only the effect of pollution on dust but also the effect of dust on accumulation mode pollution is relevant. Generally, coarse mineral dust particles transfer aerosol mass from the accumulation mode to the coarse mode by coagulation. Therefore the interaction effect on the burden of no-dust aerosol components tends to be negative for the accumulation mode but positive for the coarse mode. As Figure S11 in the supplement shows, this applies to the black carbon (BC), sea salt and water burdens. Aerosol components which interact with the mineral cations of the dust behave differently. For instance, in the

full emission simulation 1, unlike the dust free simulation 2, ammonium is driven out of the aerosol phase by the mineral cations (Metzger et al., 2006), which results in reduced aerosol ammonium burdens but increased gas phase ammonia burdens (Fig. [S11](#) [S12](#) in the supplement). This predominantly affects the accumulation mode which contains most ammonium. Conversely, the aerosol nitrate burdens are enhanced through the interaction of mineral cations with gas phase nitric acid. In contrast, [similarly](#)
5 [to non-ionic components such as BC](#), aerosol sulphate is transferred from the accumulation mode to the coarse mode through coagulation in the presence of coarse dust particles.

The changes of the accumulation mode composition reduce the hygroscopicity, the amount of accumulation mode water and the AOD. This also prolongs the atmospheric residence time of accumulation mode pollution particles in the full emission simulation 1 compared to the dust free simulation 2, increasing the burden. In comparison with the pollution free simulation 3,
10 the accumulation mode burden is enhanced by the reduced coagulation with coarse mode dust particles which are more efficiently removed in the presence of pollution. [Therefore the interaction effect on the accumulation mode dust burden is positive](#) (Fig. [S12](#) [S11](#) in the supplement). In our simulation, the effects that increase the accumulation mode burden generally outweigh the decrease due to more efficient deposition of accumulation mode dust particles. As shown in Fig. 1 (bottom), the interaction of anthropogenic pollution and dust results in an increased annual mean accumulation mode burden over most regions. [The](#)
15 [strongest increase we obtain south of the eastern part of the Sahel \(point A in Fig. 1\). The burden changes of the main aerosol components over this point which are exemplary for the whole region \(region A, cp. Table 3\) are analysed in the upper half of Fig. 2.](#) Only over some regions, most notably over Tibet ([region B in Fig. 1](#)), the decreased amount of accumulation mode water results in a decreased total [aerosol burden \(accumulation mode burden \(lower half of Fig. \[S13 in the supplement2\]\(#\)\)\)](#).

The net depleting effect of dust-pollution interactions on the coarse mode aerosol burden reduces the coarse mode contribution to the AOD, but the total AOD in the solar spectrum is dominated by the accumulation mode which is enhanced.
20 Indeed, the annual mean effect on the AOD distribution depicted at the top of Fig. 3 clearly resembles that of the effect on the accumulation mode shown at the bottom of Fig. 1 (Fig. 3 shows the AOD for the EMAC shortwave band from 250 to 690 nm including the visible wavelengths, the effect on the 550 nm AOD is practically identical, see Fig. S14 in the supplement).

The effect on the aerosol absorption optical depth (AAOD) shown at the bottom of Fig. 3 is slightly negative, due to the
25 higher reflectance and more efficient removal of aged hygroscopic coarse mode dust [and the transfer of absorbing components from accumulation to coarse mode by coagulation](#). Only south of the Sahel, where the Saharan dust mixes with biomass burning pollution, the AAOD is increased due to the strong AOD increase.

The generally reduced absorption by mineral dust interacting with pollution is also reflected in larger single scattering albedos (SSA) over dust dominated regions in simulation 1 compared to simulation 3 without anthropogenic emissions. Fig. 4

shows the annual mean difference of the SSA in both simulations. The SSA values have been averaged over the vertical levels weighted with the extinction, corresponding to using $SSA = 1 - AAOD/AOD$. Although carbonaceous components of the anthropogenic pollution reduce the SSA over the remaining globe, over the dust belt the SSA increases by up to 0.01. Together with the uncertainty of the refractive index of mineral dust, neglecting this SSA increase might be responsible for an overestimation of the atmospheric heating by dust (Balkanski et al., 2007). In the terrestrial spectrum aerosol particles are strongly absorbing corresponding to very small SSA values which are approximated by zero in the terrestrial radiative transfer code. Therefore, unlike the solar radiation, the terrestrial radiation is affected by the dust-pollution interaction only via the modified extinction.

4 Radiative forcings and heating rates

The increased AOD and decreased solar radiation absorption due to dust-pollution interactions result in a predominantly negative instantaneous direct top of the atmosphere (TOA) forcing, illustrated in Fig. 5 (top). The consequent climate cooling tendency affects large parts of the dust belt, from West Africa to East Asia, and attains an annual average of about -2 W/m^2 south of the Sahel. Positive forcings occur over Asia, exceeding 0.5 W/m^2 over India.

The distribution of the bottom of the atmosphere (BOA) forcing (Fig. 5, bottom) is similar to ~~the~~ that of the TOA forcing, with an annual mean cooling maximum south of the Sahel up to about -2.5 W/m^2 and a warming maximum over the Indo-Gangetic Plain exceeding 1 W/m^2 .

Consequently, the net atmospheric forcing is not very large, consistent with the moderate effect on the AAOD, but significant (Fig. 5, centre), and depending on the region can be either negative or positive. The largest region with atmospheric cooling extends from the Sahara over the Middle East to India, reaching an annual mean of -0.8 W/m^2 over the Arabian Peninsula. Also over the equatorial Atlantic the dust-pollution interactions result in weak but significant atmospheric cooling. In contrast, south of the Sahel the AAOD increase (see Fig. 3) results in a positive atmospheric forcing up to 0.5 W/m^2 . Over extensive regions in Asia, the forcing is positive as well, but mostly below 0.2 W/m^2 .

The TOA and BOA forcings are dominated by the effect on solar radiation (shortwave, SW, Fig. S17 in the supplement). The effect on the terrestrial radiation (longwave, LW, Fig. S18 in the supplement) ~~contributes~~ yields a forcing which is one order of magnitude smaller than the SW forcing, both globally and regionally. For the atmospheric forcing, the LW contribution is more relevant and depending on the region partially compensates or enhances the SW forcing. For example, the SW heating south of the Sahel and the SW cooling west of the Red Sea are reduced by about 30 %, whereas over the Arabian Peninsula the cooling is enhanced by about 10 %.

Through atmospheric heating and cooling dust-pollution interactions may impact regional atmospheric dynamics. In Fig. 6 we analyse the heating rates in the main regions with negative (regions 1 and 2) and positive (regions 3 and 4) annual mean atmospheric forcing. Over the largest region with net atmospheric cooling, extending from the Sahara over the Middle East to India (region 1), the heating rates show little seasonal variation with a persistent cooling, which reaches a summertime average of -0.05 K/day over the Arabian Peninsula, with a minimum during winter. Similarly, the heating over the largest region with atmospheric warming, extending from the Sahel to the Congo Basin (region 4), decreases during winter when it turns negative below 3000 m altitude.

In contrast, over regions 2 and 3 the annual average cooling and heating are largest during one season: over the equatorial Atlantic Ocean (region 2) the strongest cooling occurs during winter. Likewise, the heating over Asia is predominant during summer.

Generally, the heating takes place at higher altitudes than the cooling, at times simultaneously, thus stabilising the atmosphere, which is further intensified by the predominantly negative BOA forcing that cools the surface.

When globally averaged, the regionally positive and negative forcings partially counterbalance. Nevertheless, the net annual average global forcing at the TOA is -0.05 W/m², representing a considerable fraction of the total dust forcing: Fig. 7 compares this forcing with that of the dust when neglecting dust-pollution interactions, i.e., the dust forcing in the pollution free scenario $F_{\text{dust}} = F_3 - F_4$ which amounts to -0.08 W/m² (SW: -0.16 W/m², LW: 0.09 W/m²), and the dust forcing including the pollution effects, $F_{\text{dust}} = F_1 - F_2$, of -0.13 W/m² (SW: -0.22 W/m², LW: 0.09 W/m²). It is therefore recommended to take the interactions of dust and anthropogenic pollution into account when assessing the dust radiative forcing as they significantly enhance the net global climate cooling effect of mineral dust.

20 5 Conclusions

The physicochemical interactions of mineral dust with air pollution significantly affect the optical properties, hygroscopicity and atmospheric residence time of dust as well as anthropogenic aerosol particles. This causes an anthropogenic climate forcing linked to mineral dust, even though most of the dust itself is emitted from natural sources. ~~Competing effects on the aerosol optical properties are involved, predominantly increasing the AOD and decreasing the AAOD~~

25 Exposed to anthropogenic pollution, insoluble mineral dust particles are turned hygroscopic by chemical ageing. The subsequent hygroscopic growth increases the efficiency of scavenging and deposition, thereby reducing the atmospheric residence time and burden of coarse dust particles. This reduces the coagulation rate of accumulation mode dust particles, increasing the corresponding burden. Other aerosol components are generally transferred from the accumulation to the coarse

mode by coagulating with coarse dust particles. The interaction of ionic aerosol components with the mineral cations within the dust particles interferes with this process, driving cations such as ammonium into the gas phase or enhancing the aerosol mass of anions such as nitrate. The combined effect on the aerosol optical properties is dominated by an AOD increase caused by the enhanced accumulation mode dust burden and a decreasing AAOD due to the modified aerosol composition.

5 The resulting climate forcings are non-uniformly spatially distributed with regionally large positive and negative values. The ~~regionally negative~~ predominantly negative forcing at the top of the atmosphere over large parts of the dust belt, from West Africa to East Asia, attains a maximum of about -2 W/m^2 south of the Sahel, in contrast to a positive forcing over India. The surface forcing attains an annual mean of -2.5 W/m^2 south of the Sahel, in contrast to a mean positive forcing of 1 W/m^2 over the Indo-Gangetic Plain. The TOA forcing follows a similar pattern with slightly lower absolute values. These forcings are
10 associated with regionally and seasonally varying atmospheric cooling and heating, with persistent cooling over large parts of the dust belt from North Africa, the Arabian Peninsula to Pakistan, and heating south of the Sahel, so that a mostly stabilising impact on the atmospheric stratification is expected, which may affect the atmospheric dynamics.

Globally, dust-pollution interactions enhance the net cooling effect of mineral dust on climate. The global, annual average TOA direct radiative forcing of -0.05 W/m^2 is of similar magnitude as the ~~total dust forcing~~ dust forcing ignoring the
15 interactions, which underscores the importance of a detailed account of these interactions in the assessment of aerosol radiative forcing.

To obtain the direct forcing and to reduce the statistical noise, in the present study we have excluded feedbacks of dust and other aerosol effects on radiation transfer and clouds. These are expected to have a significant impact on atmospheric dynamics and climate, which will be the subject of a subsequent study.

20 *Code and data availability.* The Modular Earth Submodel System (MESSy) is continuously further developed and applied by a consortium of institutions. The usage of MESSy and access to the source code is licenced to all affiliates of institutions which are members of the MESSy Consortium. Institutions can become a member of the MESSy Consortium by signing the MESSy Memorandum of Understanding. More information can be found on the MESSy Consortium Website (<https://www.messy-interface.org>). The ECHAM climate model is available to the scientific community under the MPI-M Software License Agreement (<https://www.mpimet.mpg.de/en/science/models/license>). The
25 simulation results analysed in this study are archived at the German Climate Computing Centre (DKRZ) and available from the corresponding author KK until they are deposited in a public data repository.

Author contributions. KK performed the simulations assisted by VAK, analysed the model output and wrote the manuscript with support from JL who initiated the study. All authors interpreted the results and finalised the manuscript.

Competing interests. The authors declare that they have no conflict of interest.

Acknowledgements. The research reported in this publication has received funding from the King Abdullah University of Science and
5 Technology (KAUST) CRG3 grant URF/1/2180-01 *Combined Radiative and Air Quality Effects of Anthropogenic Air Pollution and Dust over the Arabian Peninsula.*

References

- Abdelkader, M., Metzger, S., Mamouri, R. E., Astitha, M., Barrie, L., Levin, Z., and Lelieveld, J.: Dust–air pollution dynamics over the eastern Mediterranean, *Atmospheric Chemistry and Physics*, 15, 9173–9189, <https://doi.org/10.5194/acp-15-9173-2015>, 2015.
- Abdelkader, M., Metzger, S., Steil, B., Klingmüller, K., Tost, H., Pozzer, A., Stenchikov, G., Barrie, L., and Lelieveld, J.: Sensitivity of transatlantic dust transport to chemical aging and related atmospheric processes, *Atmospheric Chemistry and Physics*, 17, 3799–3821, <https://doi.org/10.5194/acp-17-3799-2017>, 2017.
- Astitha, M., Lelieveld, J., Abdel Kader, M., Pozzer, A., and de Meij, A.: Parameterization of dust emissions in the global atmospheric chemistry-climate model EMAC: impact of nudging and soil properties, *Atmospheric Chemistry and Physics*, 12, 11 057–11 083, <https://doi.org/10.5194/acp-12-11057-2012>, 2012.
- 10 Balkanski, Y., Schulz, M., Claquin, T., and Guibert, S.: Reevaluation of Mineral aerosol radiative forcings suggests a better agreement with satellite and AERONET data, *Atmospheric Chemistry and Physics*, 7, 81–95, <https://doi.org/10.5194/acp-7-81-2007>, 2007.
- Bangalath, H. K. and Stenchikov, G.: Role of dust direct radiative effect on the tropical rain belt over Middle East and North Africa: A high-resolution AGCM study, *Journal of Geophysical Research: Atmospheres*, 120, 4564–4584, <https://doi.org/10.1002/2015JD023122>, 2015.
- 15 Brühl, C., Schallack, J., Klingmüller, K., Robert, C., Bingen, C., Clarisse, L., Heckel, A., North, P., and Rieger, L.: Stratospheric aerosol radiative forcing simulated by the chemistry climate model EMAC using Aerosol CCI satellite data, *Atmospheric Chemistry and Physics*, 18, 12 845–12 857, <https://doi.org/10.5194/acp-18-12845-2018>, <https://www.atmos-chem-phys.net/18/12845/2018/>, 2018.
- Clarke, L. E., Edmonds, J. A., Jacoby, H. D., Pitcher, H. M., Reilly, J. M., and Richels, R. G.: Scenarios of Greenhouse Gas Emissions and Atmospheric Concentrations. Sub-report 2.1A of Synthesis and Assessment Product 2.1 by the U.S. Climate Change Science Program and the Subcommittee on Global Change Research, 2007.
- 20 Dentener, F., Kinne, S., Bond, T., Boucher, O., Cofala, J., Generoso, S., Ginoux, P., Gong, S., Hoelzemann, J. J., Ito, A., Marelli, L., Penner, J. E., Putaud, J.-P., Textor, C., Schulz, M., van der Werf, G. R., and Wilson, J.: Emissions of primary aerosol and precursor gases in the years 2000 and 1750 prescribed data-sets for AeroCom, *Atmospheric Chemistry and Physics*, 6, 4321–4344, <https://doi.org/10.5194/acp-6-4321-2006>, <https://www.atmos-chem-phys.net/6/4321/2006/>, 2006.
- 25 Dietmüller, S., Jöckel, P., Tost, H., Kunze, M., Gellhorn, C., Brinkop, S., Frömming, C., Ponater, M., Steil, B., Lauer, A., and Hendricks, J.: A new radiation infrastructure for the Modular Earth Submodel System (MESSy, based on version 2.51), *Geoscientific Model Development*, 9, 2209–2222, <https://doi.org/10.5194/gmd-9-2209-2016>, <https://www.geosci-model-dev.net/9/2209/2016/>, 2016.
- Feng, Y. and Penner, J. E.: Global modeling of nitrate and ammonium: Interaction of aerosols and tropospheric chemistry, *Journal of Geophysical Research: Atmospheres*, 112, D01 304, <https://doi.org/10.1029/2005JD006404>, 2007.

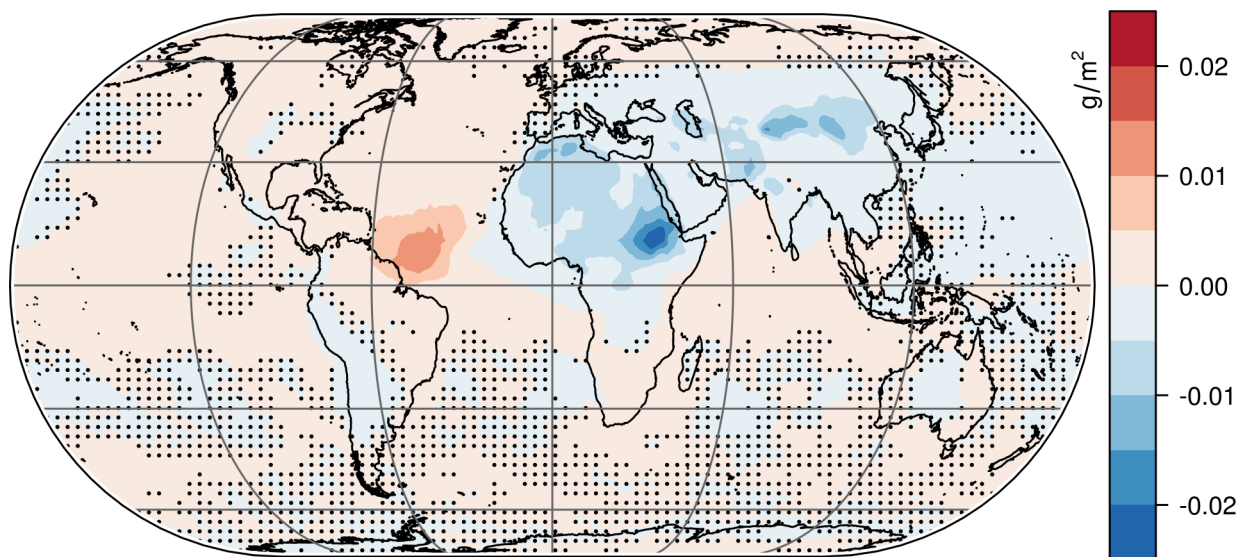
- Fountoukis, C. and Nenes, A.: ISORROPIA II: a computationally efficient thermodynamic equilibrium model for K^+ - Ca^{2+} - Mg^{2+} - NH_4^+ - Na^+ - SO_4^{2-} - NO_3^- - Cl^- - H_2O aerosols, *Atmospheric Chemistry and Physics*, 7, 4639–4659, <https://doi.org/10.5194/acp-7-4639-2007>, <http://www.atmos-chem-phys.net/7/4639/2007/>, 2007.
- Ghan, S. J., Liu, X., Easter, R. C., Zaveri, R., Rasch, P. J., Yoon, J.-H., and Eaton, B.: Toward a Minimal Representation of Aerosols in Climate Models: Comparative Decomposition of Aerosol Direct, Semidirect, and Indirect Radiative Forcing, *Journal of Climate*, 25, 6461–6476, <https://doi.org/10.1175/JCLI-D-11-00650.1>, 2012.
- Ginoux, P., Prospero, J. M., Gill, T. E., Hsu, N. C., and Zhao, M.: Global-scale attribution of anthropogenic and natural dust sources and their emission rates based on MODIS Deep Blue aerosol products, *Reviews of Geophysics*, 50, RG3005–, <https://doi.org/10.1029/2012RG000388>, 2012.
- 10 Gómez-Amo, J. L., Estellés, V., Marcos, C., Segura, S., Esteve, A. R., Pedrós, R., Utrillas, M. P., and Martínez-Lozano, J. A.: Impact of dust and smoke mixing on column-integrated aerosol properties from observations during a severe wildfire episode over Valencia (Spain), *The Science of the total environment*, 599-600, 2121–2134, <https://doi.org/10.1016/j.scitotenv.2017.05.041>, 2017.
- Hanisch, F. and Crowley, J. N.: Heterogeneous reactivity of NO and HNO₃ on mineral dust in the presence of ozone, *Physical Chemistry Chemical Physics*, 5, 883–887, <https://doi.org/10.1039/B211503D>, 2003.
- 15 Hess, M., Koepke, P., and Schult, I.: Optical Properties of Aerosols and Clouds: The Software Package OPAC., *Bulletin of the American Meteorological Society*, 79, 831–844, [https://doi.org/10.1175/1520-0477\(1998\)079<0831:OPOAAC>2.0.CO;2](https://doi.org/10.1175/1520-0477(1998)079<0831:OPOAAC>2.0.CO;2), 1998.
- Huneus, N., Schulz, M., Balkanski, Y., Griesfeller, J., Prospero, J., Kinne, S., Bauer, S., Boucher, O., Chin, M., Dentener, F., Diehl, T., Easter, R., Fillmore, D., Ghan, S., Ginoux, P., Grini, A., Horowitz, L., Koch, D., Krol, M. C., Landing, W., Liu, X., Mahowald, N., Miller, R., Morcrette, J.-J., Myhre, G., Penner, J., Perlwitz, J., Stier, P., Takemura, T., and Zender, C. S.: Global dust model intercomparison in
- 20 AeroCom phase I, *Atmospheric Chemistry and Physics*, 11, 7781–7816, <https://doi.org/10.5194/acp-11-7781-2011>, 2011.
- IPCC, ed.: *Climate Change 2013 – The Physical Science Basis*, Cambridge University Press, <http://dx.doi.org/10.1017/CBO9781107415324>, cambridge Books Online, 2014.
- Jöckel, P., Sander, R., Kerkweg, A., Tost, H., and Lelieveld, J.: Technical Note: The Modular Earth Submodel System (MESSy) - a new approach towards Earth System Modeling, *Atmospheric Chemistry and Physics*, 5, 433–444, <https://doi.org/10.5194/acp-5-433-2005>,
- 25 2005.
- Jöckel, P., Kerkweg, A., Pozzer, A., Sander, R., Tost, H., Riede, H., Baumgaertner, A., Gromov, S., and Kern, B.: Development cycle 2 of the Modular Earth Submodel System (MESSy2), *Geoscientific Model Development*, 3, 717, <https://doi.org/10.5194/gmd-3-717-2010>, 2010.
- Karydis, V. A., Tsimpidi, A. P., Lei, W., Molina, L. T., and Pandis, S. N.: Formation of semivolatile inorganic aerosols in the Mexico City Metropolitan Area during the MILAGRO campaign, *Atmospheric Chemistry and Physics*, 11, 13 305–13 323, [https://doi.org/10.5194/acp-](https://doi.org/10.5194/acp-11-13305-2011)
- 30 [11-13305-2011](https://www.atmos-chem-phys.net/11/13305/2011/), <https://www.atmos-chem-phys.net/11/13305/2011/>, 2011.
- Karydis, V. A., Tsimpidi, A. P., Pozzer, A., Astitha, M., and Lelieveld, J.: Effects of mineral dust on global atmospheric nitrate concentrations, *Atmospheric Chemistry and Physics*, 16, 1491–1509, <https://doi.org/10.5194/acp-16-1491-2016>, 2016.

- Karydis, V. A., Tsimpidi, A. P., Bacer, S., Pozzer, A., Nenes, A., and Lelieveld, J.: Global impact of mineral dust on cloud droplet number concentration, *Atmospheric Chemistry and Physics*, 17, 5601–5621, <https://doi.org/10.5194/acp-17-5601-2017>, <https://www.atmos-chem-phys.net/17/5601/2017/>, 2017.
- Kerkweg, A., Buchholz, J., Ganzeveld, L., Pozzer, A., Tost, H., and Jöckel, P.: Technical Note: An implementation of the dry removal processes DRY DEPosition and SEDimentation in the Modular Earth Submodel System (MESSy), *Atmospheric Chemistry and Physics*, 6, 4617–4632, <https://doi.org/10.5194/acp-6-4617-2006>, <https://www.atmos-chem-phys.net/6/4617/2006/>, 2006a.
- Kerkweg, A., Sander, R., Tost, H., and Jöckel, P.: Technical note: Implementation of prescribed (OFFLEM), calculated (ONLEM), and pseudo-emissions (TNUDGE) of chemical species in the Modular Earth Submodel System (MESSy), *Atmospheric Chemistry and Physics*, 6, 3603–3609, <https://doi.org/10.5194/acp-6-3603-2006>, <https://www.atmos-chem-phys.net/6/3603/2006/>, 2006b.
- 10 Kirchstetter, T. W., Novakov, T., and Hobbs, P. V.: Evidence that the spectral dependence of light absorption by aerosols is affected by organic carbon, *Journal of Geophysical Research: Atmospheres*, 109, 21 208, <https://doi.org/10.1029/2004JD004999>, 2004.
- Klingmüller, K., Steil, B., Brühl, C., Tost, H., and Lelieveld, J.: Sensitivity of aerosol radiative effects to different mixing assumptions in the AEROPT 1.0 submodel of the EMAC atmospheric-chemistry–climate model, *Geoscientific Model Development*, 7, 2503–2516, <https://doi.org/10.5194/gmd-7-2503-2014>, <https://www.geosci-model-dev.net/7/2503/2014/>, 2014.
- 15 Klingmüller, K., Pozzer, A., Metzger, S., Stenchikov, G. L., and Lelieveld, J.: Aerosol optical depth trend over the Middle East, *Atmospheric Chemistry and Physics*, 16, 5063–5073, <https://doi.org/10.5194/acp-16-5063-2016>, <https://www.atmos-chem-phys.net/16/5063/2016/>, 2016.
- Klingmüller, K., Metzger, S., Abdelkader, M., Karydis, V. A., Stenchikov, G. L., Pozzer, A., and Lelieveld, J.: Revised mineral dust emissions in the atmospheric chemistry–climate model EMAC (MESSy 2.52 DU_Astitha1 KKDU2017 patch), *Geoscientific Model Development*, 20 11, 989–1008, <https://doi.org/10.5194/gmd-11-989-2018>, <https://www.geosci-model-dev.net/11/989/2018/>, 2018.
- Koepke, P., Gasteiger, J., and Hess, M.: Technical Note: Optical properties of desert aerosol with non-spherical mineral particles: data incorporated to OPAC, *Atmospheric Chemistry and Physics*, 15, 5947–5956, <https://doi.org/10.5194/acp-15-5947-2015>, 2015.
- Kok, J. F., Ridley, D. A., Zhou, Q., Miller, R. L., Zhao, C., Heald, C. L., Ward, D. S., Albani, S., and Haustein, K.: Smaller desert dust cooling effect estimated from analysis of dust size and abundance, *Nature Geoscience*, 10, 274–278, <https://doi.org/10.1038/ngeo2912>, 2017.
- 25 Lauer, A., Eyring, V., Hendricks, J., Jöckel, P., and Lohmann, U.: Global model simulations of the impact of ocean-going ships on aerosols, clouds, and the radiation budget, *Atmospheric Chemistry and Physics*, 7, 5061–5079, <https://doi.org/10.5194/acp-7-5061-2007>, <https://www.atmos-chem-phys.net/7/5061/2007/>, 2007.
- Lelieveld, J., Evans, J. S., Fnais, M., Giannadaki, D., and Pozzer, A.: The contribution of outdoor air pollution sources to premature mortality on a global scale, *Nature*, 525, 367–371, <https://doi.org/10.1038/nature15371>, 2015.
- 30 Levin, Z., Ganor, E., and Gladstein, V.: The Effects of Desert Particles Coated with Sulfate on Rain Formation in the Eastern Mediterranean., *Journal of Applied Meteorology*, 35, 1511–1523, [https://doi.org/10.1175/1520-0450\(1996\)035<1511:TEODPC>2.0.CO;2](https://doi.org/10.1175/1520-0450(1996)035<1511:TEODPC>2.0.CO;2), 1996.

- Levine, J.: 5.5 - Biomass Burning: The Cycling of Gases and Particulates from the Biosphere to the Atmosphere, in: *Treatise on Geochemistry (Second Edition)*, edited by Holland, H. D. and Turekian, K. K., pp. 139 – 150, Elsevier, Oxford, second edition edn., <https://doi.org/https://doi.org/10.1016/B978-0-08-095975-7.00405-8>, <http://www.sciencedirect.com/science/article/pii/B9780080959757004058>, 2014.
- 5 MESSy 2018: MESSy submodel list, http://www.messy-interface.org/current/auto/messy_submodels.html, visited 1 April 2018.
- Metzger, S., Mihalopoulos, N., and Lelieveld, J.: Importance of mineral cations and organics in gas-aerosol partitioning of reactive nitrogen compounds: case study based on MINOS results, *Atmospheric Chemistry and Physics*, 6, 2549–2567, <https://doi.org/10.5194/acp-6-2549-2006>, <https://www.atmos-chem-phys.net/6/2549/2006/>, 2006.
- Metzger, S., Steil, B., Abdelkader, M., Klingmüller, K., Xu, L., Penner, J. E., Fountoukis, C., Nenes, A., and Lelieveld, J.: Aerosol water
10 parameterisation: a single parameter framework, *Atmospheric Chemistry and Physics*, 16, 7213–7237, <https://doi.org/10.5194/acp-16-7213-2016>, <http://www.atmos-chem-phys.net/16/7213/2016/>, 2016.
- Osipov, S. and Stenchikov, G.: Simulating the Regional Impact of Dust on the Middle East Climate and the Red Sea, *Journal of Geophysical Research: Oceans*, 123, 1032–1047, <https://doi.org/10.1002/2017JC013335>, 2018.
- Osipov, S., Stenchikov, G., Brindley, H., and Banks, J.: Diurnal cycle of the dust instantaneous direct radiative forcing over the Arabian
15 Peninsula, *Atmospheric Chemistry and Physics*, 15, 9537–9553, <https://doi.org/10.5194/acp-15-9537-2015>, 2015.
- Pozzer, A., de Meij, A., Pringle, K. J., Tost, H., Doering, U. M., van Aardenne, J., and Lelieveld, J.: Distributions and regional budgets of aerosols and their precursors simulated with the EMAC chemistry-climate model, *Atmospheric Chemistry and Physics*, 12, 961–987, <https://doi.org/10.5194/acp-12-961-2012>, <https://www.atmos-chem-phys.net/12/961/2012/>, 2012.
- Pringle, K. J., Tost, H., Message, S., Steil, B., Giannadaki, D., Nenes, A., Fountoukis, C., Stier, P., Vignati, E., and Lelieveld, J.: De-
20 scription and evaluation of GMXe: a new aerosol submodel for global simulations (v1), *Geoscientific Model Development*, 3, 391, <https://doi.org/10.5194/gmd-3-391-2010>, 2010a.
- Pringle, K. J., Tost, H., Metzger, S., Steil, B., Giannadaki, D., Nenes, A., Fountoukis, C., Stier, P., Vignati, E., and Lelieveld, J.: Corrigendum to “Description and evaluation of GMXe: a new aerosol submodel for global simulations (v1)” published in *Geosci. Model Dev.*, 3, 391–412, 2010, *Geoscientific Model Development*, 3, 413, <https://doi.org/10.5194/gmd-3-413-2010>, 2010b.
- 25 Raes, F. and Van Dingenen, R.: Simulations of condensation and cloud condensation nuclei from biogenic SO₂ in the remote marine boundary layer, *Journal of Geophysical Research*, 97, 12 901, <https://doi.org/10.1029/92JD00961>, 1992.
- Randerson, J., van der Werf, G., Giglio, L., Collatz, G., and Kasibhatla, P.: Global Fire Emissions Database, Version 3 (GFEDv3.1), <https://doi.org/10.3334/ORNLDAAC/1191>, 2013.
- Ridley, D. A., Heald, C. L., Kok, J. F., and Zhao, C.: An observationally constrained estimate of global dust aerosol optical depth, *Atmospheric
30 Chemistry and Physics*, 16, 15 097–15 117, <https://doi.org/10.5194/acp-16-15097-2016>, 2016.
- Rothman, L. S., Jacquemart, D., Barbe, A., Chris Benner, D., Birk, M., Brown, L. R., Carleer, M. R., Chackerian, C., Chance, K., Coudert, L. H., Dana, V., Devi, V. M., Flaud, J.-M., Gamache, R. R., Goldman, A., Hartmann, J.-M., Jucks, K. W., Maki, A. G., Mandin, J.-Y.,

- Massie, S. T., Orphal, J., Perrin, A., Rinsland, C. P., Smith, M. A. H., Tennyson, J., Tolchenov, R. N., Toth, R. A., Vander Auwera, J., Varanasi, P., and Wagner, G.: The HITRAN 2004 molecular spectroscopic database, *Journal of Quantitative Spectroscopy and Radiative Transfer*, 96, 139, <https://doi.org/10.1016/j.jqsrt.2004.10.008>, 2005.
- Sander, R., Baumgaertner, A., Gromov, S., Harder, H., Jöckel, P., Kerkweg, A., Kubistin, D., Regelin, E., Riede, H., Sandu, A., Taraborrelli, D., Tost, H., and Xie, Z.-Q.: The atmospheric chemistry box model CAABA/MECCA-3.0, *Geoscientific Model Development*, 4, 373–380, <https://doi.org/10.5194/gmd-4-373-2011>, <https://www.geosci-model-dev.net/4/373/2011/>, 2011.
- Stier, P., Feichter, J., Kinne, S., Kloster, S., Vignati, E., Wilson, J., Ganzeveld, L., Tegen, I., Werner, M., Balkanski, Y., Schulz, M., Boucher, O., Minikin, A., and Petzold, A.: The aerosol-climate model ECHAM5-HAM, *Atmospheric Chemistry and Physics*, 5, 1125–1156, <https://doi.org/10.5194/acp-5-1125-2005>, 2005.
- 10 Tanre, D., Geleyn, J.-F., and Slingo, J. M.: First results of the introduction of an advanced aerosol-radiation interaction in the ECMWF low resolution global model, in: *Aerosols and their climatic effects*, edited by Gerber, H. and Deepak, A., pp. 133–177, A. Deepak Pub., 1984.
- Tost, H., Jöckel, P., Kerkweg, A., Sander, R., and Lelieveld, J.: Technical note: A new comprehensive SCAVenging submodel for global atmospheric chemistry modelling, *Atmospheric Chemistry and Physics*, 6, 565–574, <https://doi.org/10.5194/acp-6-565-2006>, <https://www.atmos-chem-phys.net/6/565/2006/>, 2006.
- 15 Tsimpidi, A. P., Karydis, V. A., Pozzer, A., Pandis, S. N., and Lelieveld, J.: ORACLE (v1.0): module to simulate the organic aerosol composition and evolution in the atmosphere, *Geoscientific Model Development*, 7, 3153–3172, <https://doi.org/10.5194/gmd-7-3153-2014>, <https://www.geosci-model-dev.net/7/3153/2014/>, 2014.
- Van Doren, J. M., Watson, L. R., Davidovits, P., Worsnop, D. R., Zahniser, M. S., and Kolb, C. E.: Temperature dependence of the uptake coefficients of nitric acid, hydrochloric acid and nitrogen oxide (N₂O₅) by water droplets, *The Journal of Physical Chemistry*, 94, 3265–3269, <https://doi.org/10.1021/j100371a009>, 1990.
- 20 Vignati, E., Wilson, J., and Stier, P.: M7: An efficient size-resolved aerosol microphysics module for large-scale aerosol transport models, *Journal of Geophysical Research: Atmospheres*, 109, D22 202, <https://doi.org/10.1029/2003JD004485>, 2004.
- Yue, X., Wang, H., Liao, H., and Fan, K.: Direct climatic effect of dust aerosol in the NCAR Community Atmosphere Model Version 3 (CAM3), *Advances in Atmospheric Sciences*, 27, 230–242, <https://doi.org/10.1007/s00376-009-8170-z>, 2010.

Δ coarse mode burden



Δ accumulation mode burden

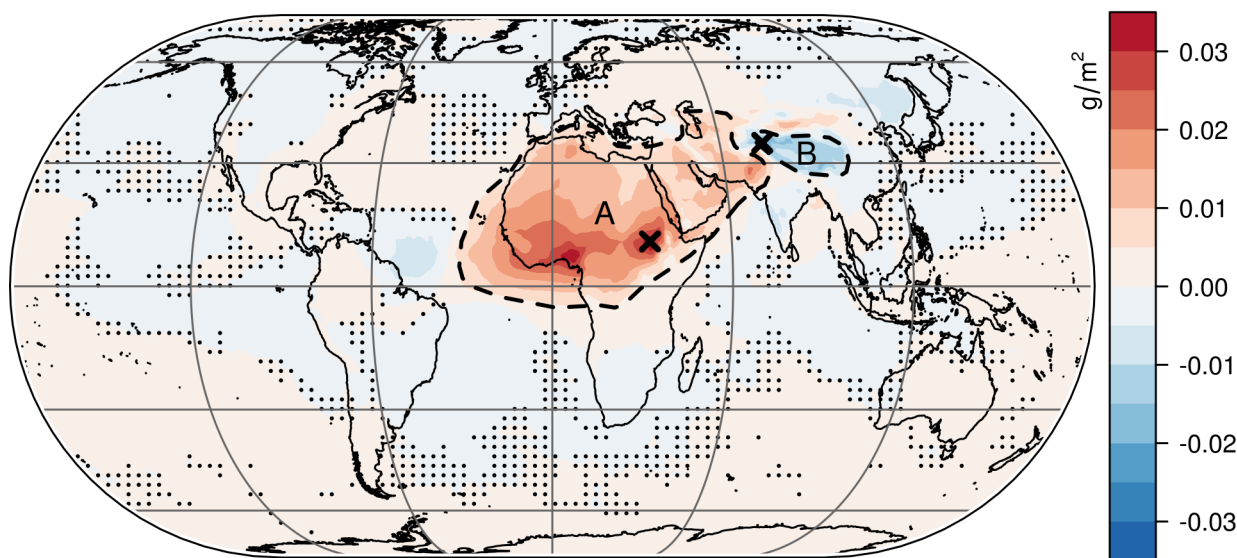


Figure 1. Impact of dust-pollution interaction on the coarse mode (top) and accumulation mode (bottom) aerosol burden (including aerosol water). The more efficient removal of aged dust particles reduces the coarse mode burden throughout the dust belt. This in turn reduces the coagulation efficiency of coarse mode with smaller particles, increasing the accumulation mode burden especially where the dust and the African biomass burning regions coincide. The strong hygroscopic growth of aged Saharan dust particles over the western Atlantic results in a regional maximum of the coarse mode burden increase. Generally, the hygroscopic growth of accumulation mode particles is reduced by the interaction with mineral dust cations manifested in a decreased accumulation mode burden over Tibet. The burdens over points A and B (crosses) are analysed in Fig. 2, relevant variables over regions A and B in Table 3 and Fig. S13. Dots indicate regions where the effect of the dust-pollution interaction is insignificant.

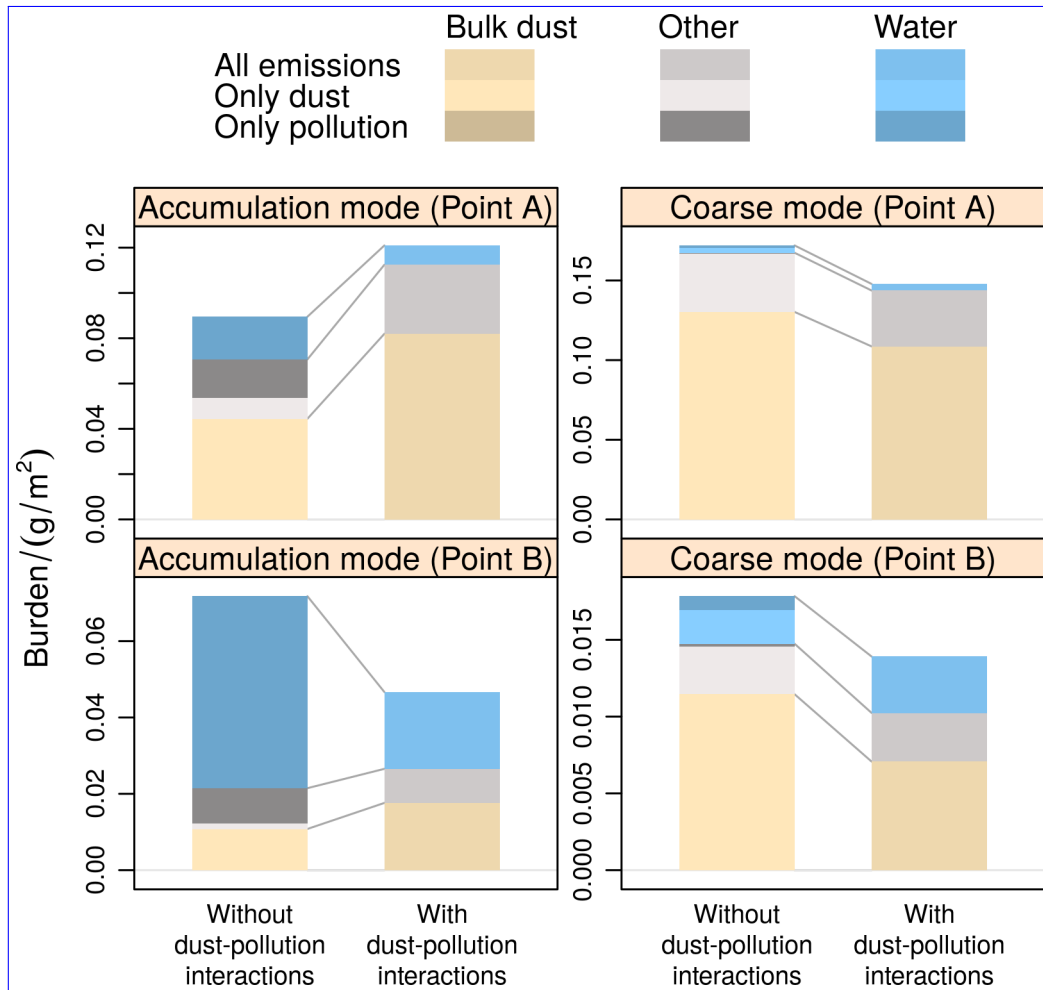


Figure 2. Analysis of the interaction effect on the aerosol mass burden over point A (top) and point B (bottom) in Fig. 1. The left bar in each panel represents the burden of non-interacting dust and pollution. It corresponds to $(F_2 - F_4) + (F_3 - F_4)$ in Eq. (2), stacking the burdens in simulation 2 with only pollution and simulation 3 with only dust, each after subtracting the background burdens from simulation 4 without dust and pollution. The right bar in each panel represents the burden of interacting dust and pollution in simulation 1 (after subtracting the background burden) corresponding to $F_1 - F_4$ in Eq. (2).

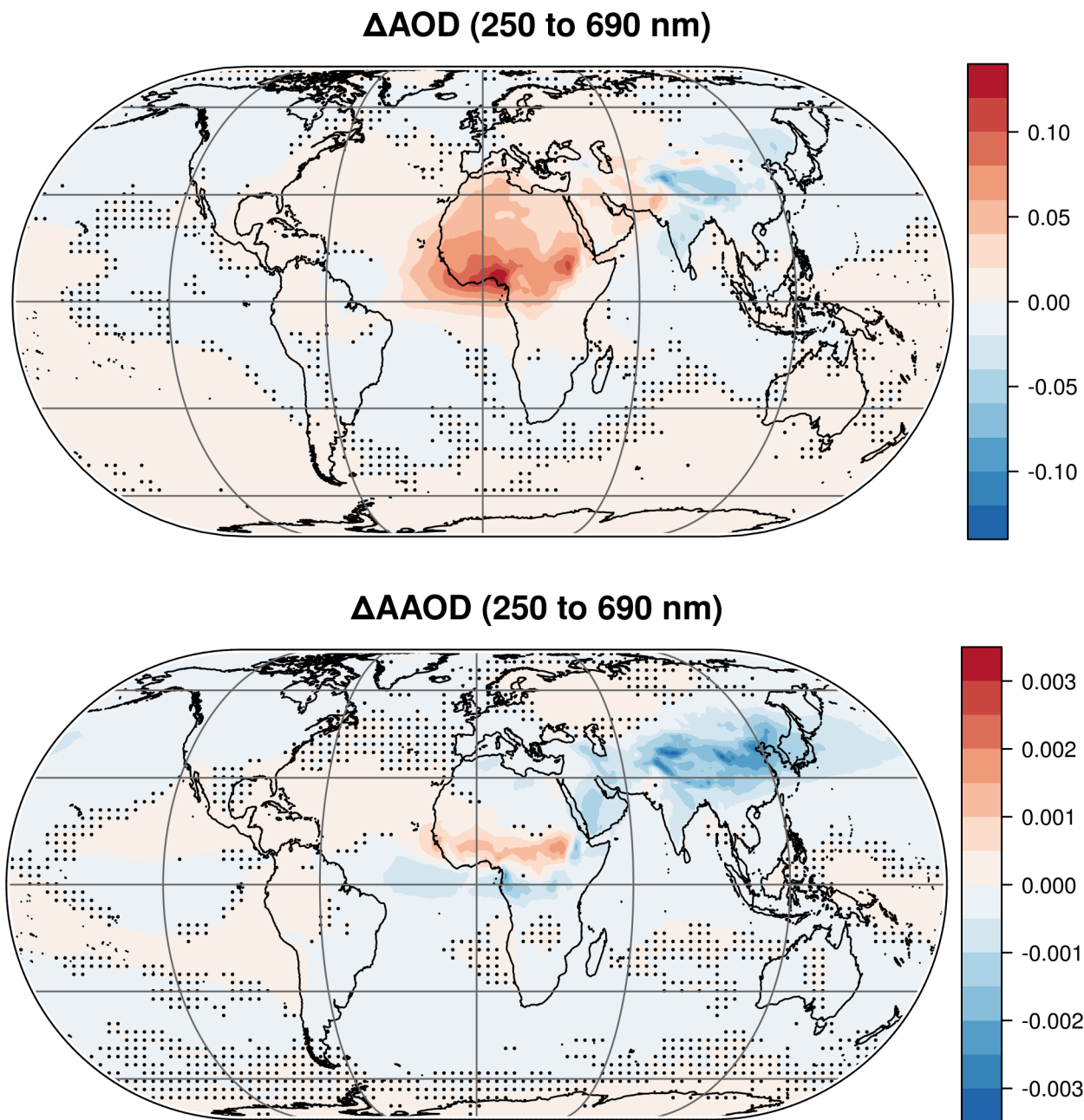


Figure 3. Impact of dust-pollution interaction on the AOD (top) and the absorption AOD (AAOD, bottom). The AOD change reflects the changes of the accumulation mode burden shown in Fig. 1. Over large parts of the dust belt the accumulation mode AOD is increased. In contrast, over the Tibetan Plateau and east India the AOD decreases due to reduced hygroscopic growth of accumulation mode particles. South of the Sahel, where the Saharan dust mixes with biomass burning pollution, the strongest accumulation mode AOD and AAOD increase occurs. Elsewhere, the water uptake of dust and the more efficient removal of absorbing coarse dust particles combined with the changed accumulation mode ~~partiele~~ ~~particle~~ radii and refractive indices tend to decrease the AAOD. Dots indicate regions where the effect of the dust-pollution interaction is insignificant. Figure S15 in the supplement shows the corresponding plots for the four seasons.

Δ SSA (with - without pollution) (250 to 690 nm)

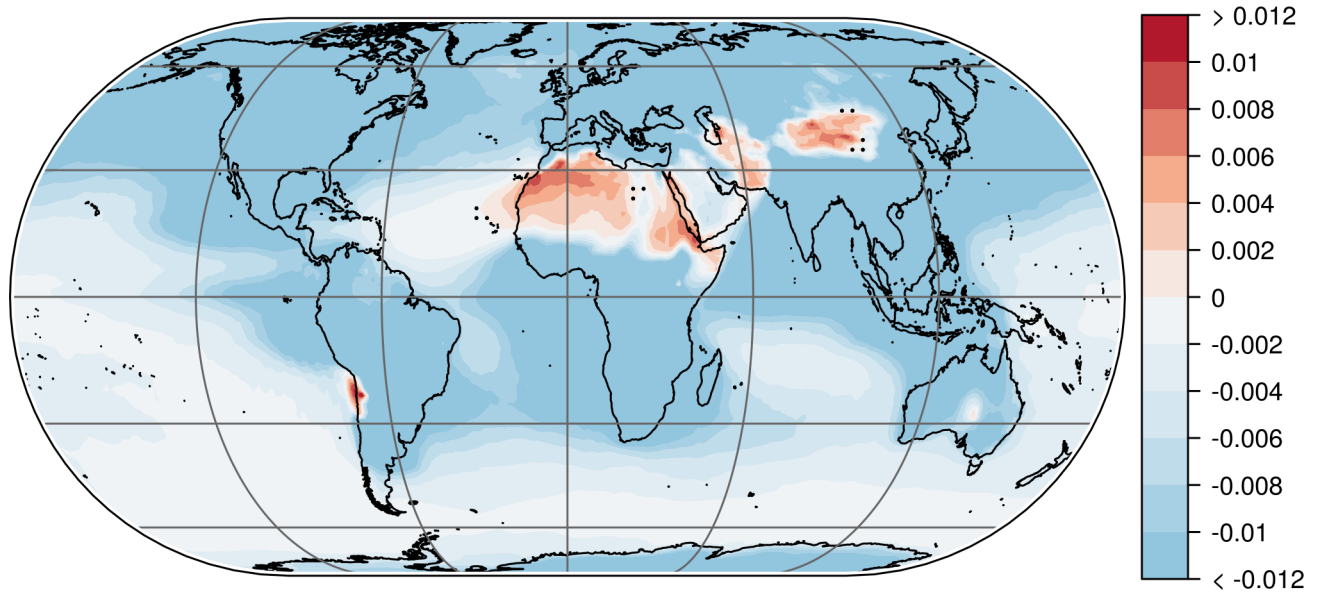


Figure 4. Annual mean difference of the single scattering albedo (SSA) with (simulation 1) and without (simulation 3) anthropogenic emissions. Extinction weighted mean SSA values of each vertical column are used. The SSA for all four emission setups is shown in Fig. S16 in the supplement. Dots indicate regions where the difference is insignificant.

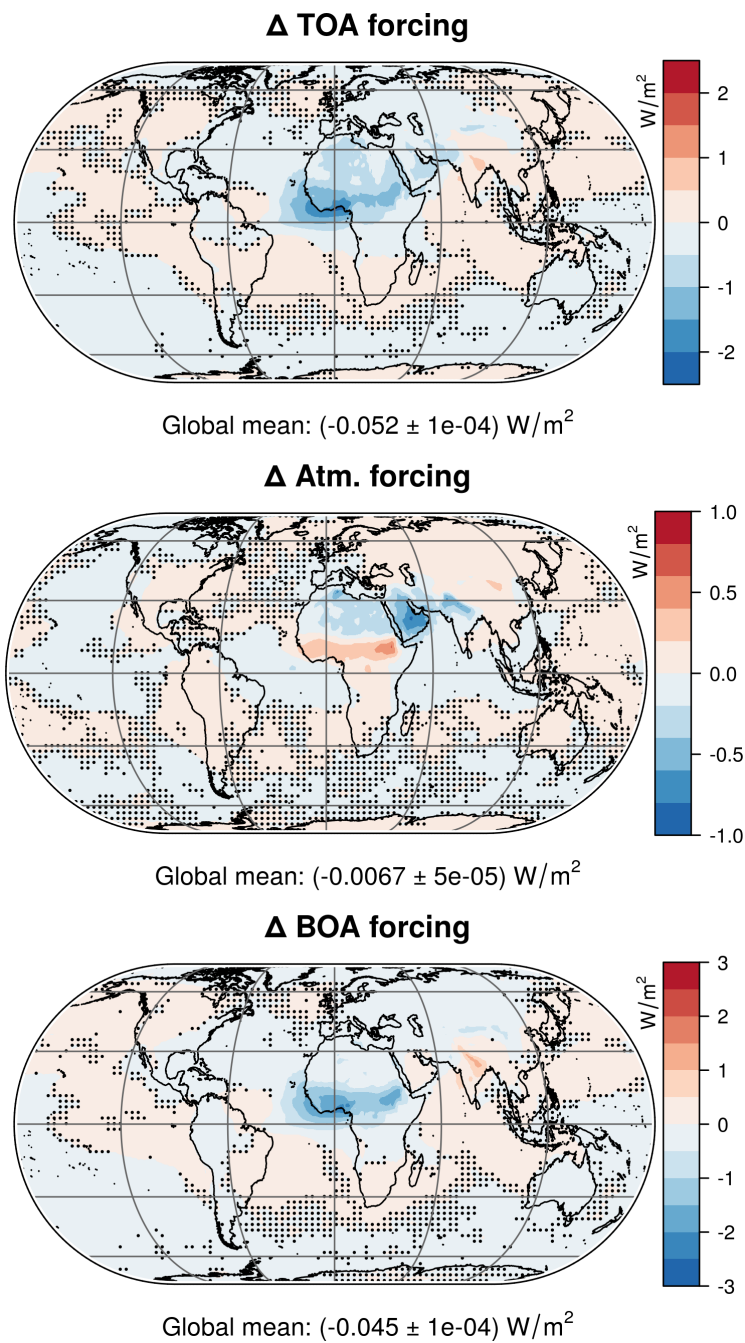


Figure 5. The instantaneous total (solar and terrestrial) direct radiative forcing of the dust-pollution interaction at the top of the atmosphere (TOA, top), within the atmosphere (centre) and at the bottom of the atmosphere (BOA, bottom). Dots indicate regions where the effect of the dust-pollution interaction is insignificant. The corresponding figures showing the solar and terrestrial forcings as well as seasonality are provided in the supplement (Figs. S17 to S19).

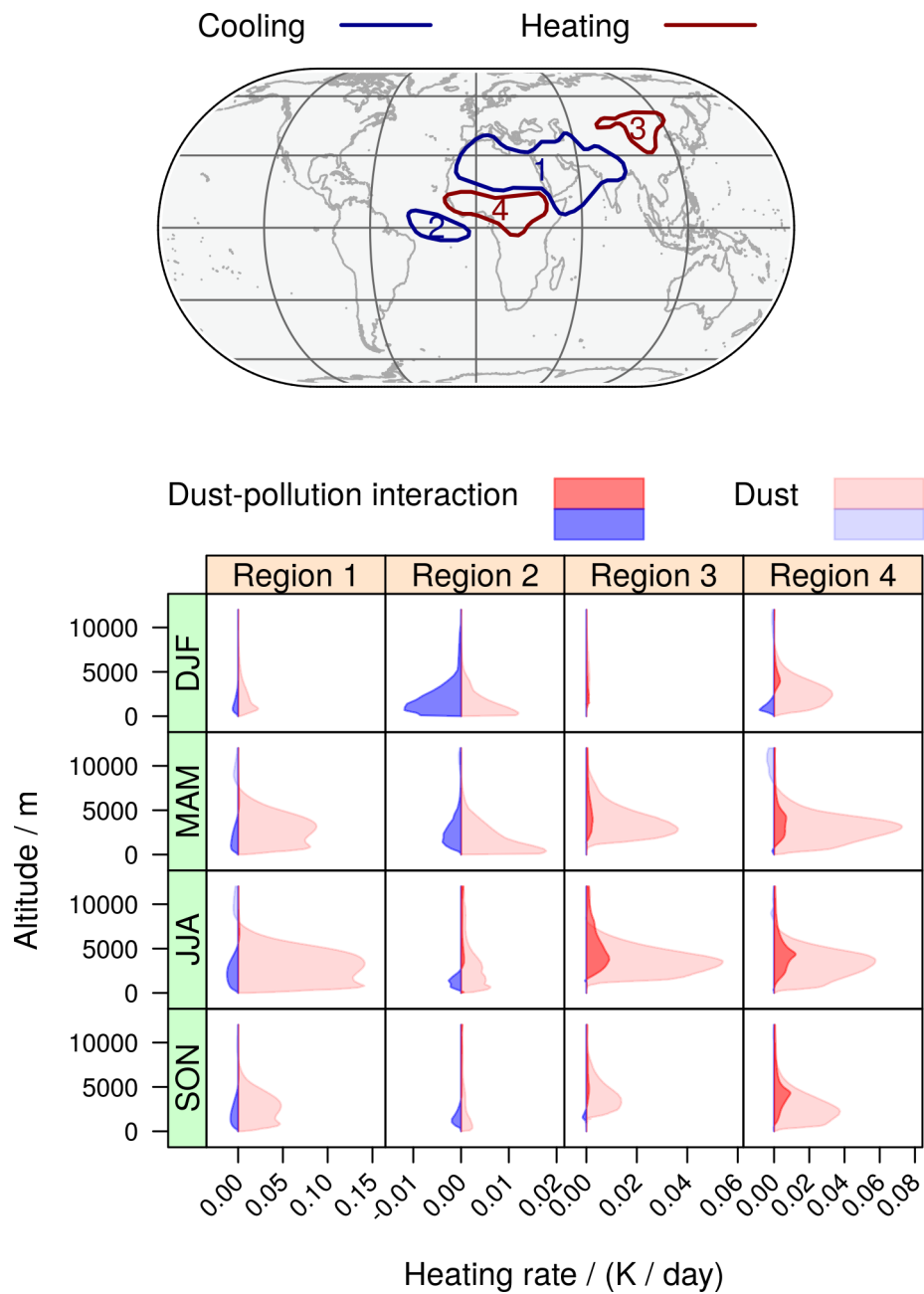


Figure 6. Heating rate contribution of dust-pollution interaction-interactions (rich colours) in comparison with the mineral dust contribution (pale colours). Seasonal heating rate profiles of four regions with negative (regions 1 and 2) and positive (regions 3 and 4) annual mean atmospheric forcing are shown (bottom). The regions (top) are selected based on the forcings displayed in the centre of Fig. 5, using regions where the absolute forcing exceeds 0.1 W/m^2 after applying a Gaussian filter to avoid fragmentation. Three-dimensional isosurfaces of the seasonal heating rates are presented in the supplement (Figs. S20 to S23).

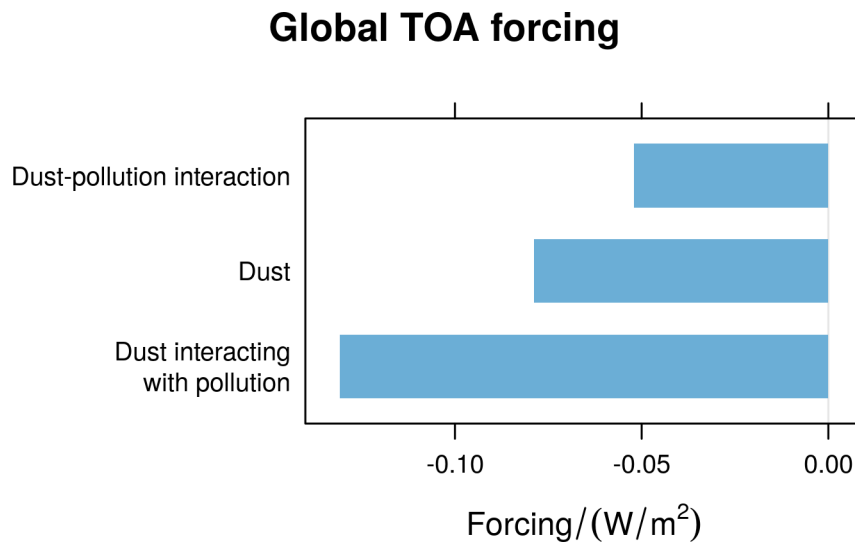


Figure 7. Global mean top of the atmosphere (TOA) forcing of the dust-pollution interaction in comparison with the mineral dust forcing from the same EMAC simulation excluding/including the dust-pollution interaction. The CVs of the interannual variation are (from top to bottom) 7 %, 6 % and 5 %.

Table 1. Emission setups

Simulation	1	2	3	4
Anthropogenic emissions	yes	yes	no	no
Dust emissions	yes	no	yes	no

Table 2. Accommodation coefficients

Gas-phase species	Accommodation coefficient	References
Sulfuric acid (H ₂ SO ₄)	0.3 (on insoluble particles)	M7 (Vignati et al., 2004), Raes and Van Dingenen (1992)
	1 (on soluble particles)	M7 (Vignati et al., 2004)
Nitric acid (HNO ₃)	0.1	GMXE (Pringle et al., 2010a, b), Hanisch and Crowley (2003)
Hydrochloric acid (HCl)	0.064	GMXE (Pringle et al., 2010a, b), Van Doren et al. (1990)
Ammonia (NH ₃)	0.097	GMXE (Pringle et al., 2010a, b), Feng and Penner (2007)
Water (H ₂ O)	0.3 (on insoluble particles)	GMXE (Pringle et al., 2010a, b)
	1 (on soluble particles)	GMXE (Pringle et al., 2010a, b)

Table 3. Annual mean results for various variables over regions A and B in Fig. 1 and the included contributions Δ of the dust-pollution interactions.

Variable	Region A		Region B		Unit
	Value	Δ	Value	Δ	
AOD (250 to 690 nm)	0.38	0.042	0.16	-0.047	
AAOD (250 to 690 nm)	0.029	-0.00017	0.0094	-0.0017	
Dust forcing, pollution forcing	-0.35, -1.2	-0.68	0.072, -0.20	0.13	W / m ²
Mineral dust burden (accumulation mode)	0.042	0.013	0.011	0.0045	$\mu\text{g} / \text{m}^3$
Mineral dust burden (coarse mode)	0.096	-0.0073	0.0061	-0.0024	$\mu\text{g} / \text{m}^3$
BC burden (accumulation mode)	0.00034	-8.3e-05	0.00021	-3.1e-05	$\mu\text{g} / \text{m}^3$
BC burden (coarse mode)	6.8e-05	2.3e-05	2.9e-05	1.2e-05	$\mu\text{g} / \text{m}^3$
Sea salt burden (accumulation mode)	0.0028	-0.00064	0.00030	-3.5e-05	$\mu\text{g} / \text{m}^3$
Sea salt burden (coarse mode)	0.0030	0.00019	6.6e-05	-1.6e-05	$\mu\text{g} / \text{m}^3$
Aerosol water burden (accumulation mode)	0.018	-0.0011	0.023	-0.015	$\mu\text{g} / \text{m}^3$
Aerosol water burden (coarse mode)	0.011	0.0016	0.0040	-0.00029	$\mu\text{g} / \text{m}^3$